Carboxylate as the Protonation Site in (Peroxo)diiron(III) Model Complexes of Soluble Methane Monooxygenase and Related Diiron Proteins

ARTICLE *in* JOURNAL OF THE AMERICAN CHEMICAL SOCIETY · FEBRUARY 2010

Impact Factor: 12.11 · DOI: 10.1021/ja909718f · Source: PubMed

4 AUTHORS, INCLUDING:

Pierre Moënne-Loccoz
Oregon Health and Science University
109 PUBLICATIONS **3,191** CITATIONS

SEE PROFILE

Published in final edited form as:
J Am Chem Soc. 2010 February 3; 132(4): 1273–1275. doi:10.1021/ja909718f.

Carboxylate as the Protonation Site in (Peroxo)diiron(III) Model Complexes of Soluble Methane Monooxygenase and Related Diiron Proteins

Loi H. Do[†], **Takahiro Hayashi**[§], **Pierre Moënne-Loccoz**[*,§], and **Stephen J. Lippard**[*,†]

[†]Department of Chemistry, Massachusetts Institute of Technology, Cambridge, MA 02139

[§]Department of Science and Engineering, School of Medicine, Oregon Health and Science University, Beaverton, OR 97006

Abstract

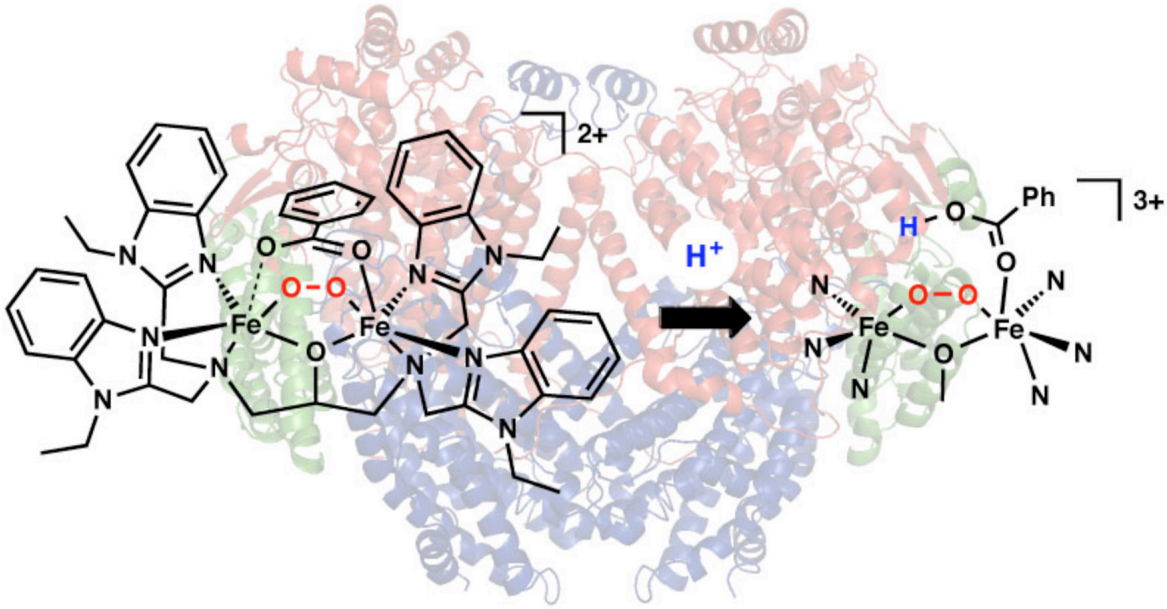

Addition of H^+ to a synthetic (μ-1,2-peroxo)diiron(III) model complex results in protonation of a carboxylate rather than the peroxo ligand. This conclusion is based on spectroscopic evidence from UV-vis, ^{57}Fe Mössbauer, resonance Raman, infrared, and ^{1}H/^{19}F NMR studies. These results suggest a similar role for protons in the dioxygen activation reactions in soluble methane monooxygenase and related carboxylate-bridged diiron enzymes.

Dioxygen activation by carboxylate-bridged diiron enzymes is involved in essential biological processes[1,2] ranging from DNA synthesis and hydrocarbon metabolism to cell proliferation.[3] The carboxylate-bridged diiron superfamily of proteins includes ribonucleotide reductase

ploccoz@ebs.ogi.edu; lippard@mit.edu.

Supporting Information Available. Synthesis and characterization of diiron(II) complexes, experimental procedures, and spectroscopic data. This material is available free of charge via the Internet at http://pubs.acs.org.

(RNR),[4] Δ^9 desaturase,5 bacterial multicomponent monooxygenases (BMMs),6,7 and most recently human deoxyhypusine hydroxylase (hDOHH).3 In all of these systems, the O_2 reduction step proceeds through a (peroxo)diiron(III) intermediate in which the resulting peroxo ligand is proposed to bridge two iron atoms in a μ-1,2 or μ-η^2 η^2 coordination mode.[8–10] Extensive studies of soluble methane monooxygenase (sMMO), a BMM family member that oxidizes methane to methanol, reveal that the generation and activation of Fe_2O_2 units requires protons.[11,12] Given the complexity of protein environments, identifying the sites involved in such proton translocation processes and their effect on O_2 activation is not a trivial undertaking.

To shed light on the possible role of protons in the dioxygen activation chemistry at carboxylate-bridged diiron enzyme active sites, we investigated the reaction of H^+ with a well-characterized synthetic (μ-peroxo)(μ-carboxylato)diiron(III) complex, $[Fe_2(\mu\text{-}O_2)(N\text{-EtHPTB})(\mu\text{-}PhCO_2)]^{2+}$ (**1a**·O_2).[13,14] The dinucleating *N*-EtHPTB ligand provides kinetic stabilization of the Fe_2O_2 core and the benzoate group serves as a good mimic of the Asp and Glu carboxylate side chains in the protein diiron centers. By application of several spectroscopic methods, we show that the reaction of H^+ with **1a**·O_2 results in protonation at the carboxylate unit rather than the peroxo ligand (Scheme 1). This work provides experimental support for recent theoretical studies suggesting that (hydroperoxo)-diiron(III) species of non-heme diiron enzymes are too reactive to be isolable protein intermediates.[15]

To aid spectral interpretation of results obtained during studies of the parent $[Fe_2(N\text{-EtHPTB})(\mu\text{-}PhCO_2)]^{2+}$ complex (**1a**), two related diiron(II) precursors were synthesized (Supporting Information). One is $[Fe_2(N\text{-EtHPTB})\text{-}(Ph^{13}CO_2)]^{2+}$ (**1b**), which contains a ^{13}C-enriched carboxylate ligand, and the other is $[Fe_2(N\text{-EtHPTB})(C_6F_5CO_2)]^{2+}$ (**2**), in which the benzoate ring is fluorinated.

Exposure of **1a** to O_2 in CH_3CN at −30 °C generates a deep blue-green solution (**1a**·O_2) with λ_{max} at 590 nm.[13] Addition of an acetonitrile solution of $[H(OEt_2)_2][3,5\text{-}(CF_3)_2C_6H_3)_4B]$ (H[BAr^F_4]) to **1a**·O_2 red-shifts the peroxo-to-iron(III) charge transfer band to ~600 nm (Fig. 1). This absorption is assigned to the formation of a new [**1a**·O_2]H^+ species that maximizes with addition of ~1.5 equiv of H[BAr^F_4]. The spectrum of **1a**·O_2 is restored upon addition of 2.0 equiv of NEt_3 (Fig. 1, inset), indicating that protonation does not lead to irreversible decomposition of the **1a**·O_2 unit. Reaction of **2** with O_2 affords $[Fe_2(\mu\text{-}O_2)(N\text{-EtHPTB})(\mu\text{-}C_6F_5CO_2)]^{2+}$ (**2**·O_2), which exhibits a broad absorption feature centered at ~600 nm. When H[BAr^F_4] was titrated into a solution of **2**·O_2, a small bathochromic shift to ~610 nm occurs (Fig. S1). Unlike **1a**·O_2, **2**·O_2 requires ~3.0 equiv of H[BAr^F_4]. to fully generate the protonated species [**2**·O_2]H^+. Given that pentafluorobenzoate, for which the acid has a pK_a of 1.2, is more electron deficient than benzoate (acid pK_a = 4.6), the greater amount of H^+ necessary to produce [**2**·O_2]H^+ from **2**·O_2 compared to [**1a**·O_2]H^+ from **1a**·O_2 suggests either that the carboxylate ligand influences the basicity of the protonation site or that it is itself the proton acceptor.

To determine whether a (hydroperoxo)diiron(III) species may form upon addition of H^+ to **1a**·O_2 or **2**·O_2, ^{57}Fe Mössbauer and resonance Raman (RR) spectra were recorded to examine possible changes in the Fe_2O_2 core. In the absence of H^+, the Mössbauer spectrum of a frozen solution of **1a**·O_2 in CH_3CN could be fit to a single iron site, with δ = 0.53(2) mm/s and ΔE_Q = 0.71(2) mm/s (Fig. S2A). Addition of H[BAr^F_4]. to **1a**·O_2 gives [**1a**·O_2]H^+ having the same isomer shift (δ = 0.53(2) mm/s) and a slightly larger quadrupole splitting parameter (ΔE_Q = 0.80(2) mm/s) (Fig. S2B). For comparison, the Mössbauer spectra of **2**·O_2 and [**2**·O_2]H^+ were also recorded. The (peroxo)diiron(III) complex of **2** has δ = 0.53(2) mm/s and ΔE_Q = 0.77(2) mm/s (Fig. S2C), whereas the protonated [**2**·O_2]H^+ form exhibits parameters of δ = 0.54(2) mm/s and ΔE_Q = 0.84(2) mm/s (Fig. S2D). The similar isomer shifts obtained for **1a**·O_2, [**1a**·O_2]H^+, **2**·O_2, and [**2**·O_2]H^+ are indicative of iron(III) centers and the small increase

in ΔE_Q values for the protonated forms implies that only minor changes occur in the coordination environment.

To investigate more directly the nature of the peroxo moiety, Fe–O and O–O vibrations were measured by RR spectroscopy for species generated with both $^{16}O_2$ and $^{18}O_2$. As previously reported,[13] **1a**·O_2 exhibits Fe–O and O–O stretching vibrations with Fermi splitting (hereafter "/") centered at 470 and 897 cm^{-1}, respectively (Fig. S3). Also observed are weaker bands at 513/532 cm^{-1} that downshift to 500 cm^{-1} with $^{18}O_2$, which we therefore assign to the asymmetric Fe–O stretch of the Fe_2O_2 core. Addition of H^+ to **1a**·O_2 only marginally affects its RR spectrum, with small upshift in Fe–O and downshift in O–O vibrations (Fig. S3, Table 1). These shifts in RR frequencies upon H^+ addition may reflect subtle changes in Fe–O–O–Fe angles,[16] but are too small to support the conclusion that a (μ-1,2-peroxo)diiron(III) unit has been converted to a (hydroperoxo)diiron(III) species. The RR spectrum of **2**·O_2 is practically identical to that of **1a**·O_2, with symmetric and asymmetric Fe–O modes at 466/475 and 513/532 cm^{-1}, respectively, and Fermi-coupled O–O stretches centered at 897 cm^{-1} (Fig. 2). Addition of up to 2.0 equiv of H[BAr^F_4] to generate [**2**·O_2]H^+ primarily affects the symmetric Fe–O stretch, which upshifts only a few wavenumbers compared to the spectrum of **2**·O_2 (Table 1). From the RR data and Mössbauer parameters for **1a**·O_2, [**1a**·O_2]H^+, **2**·O_2, and [**2**·O_2]H^+, we conclude that protonation does not lead to formation of a (hydroperoxo) diiron(III) species.

Since the benzimidazole and propoxy groups of *N*-EtHPTB are kinetically inaccessible due to the multidentate nature of the ligand, we assign the carboxylate unit as the site of protonation. To test this hypothesis, we examined the carboxylate stretches of **1a** and **1b**, and their peroxo complexes by FTIR spectroscopy. The assignment of frequencies in terms of coordination geometry are complicated by mixing of the COO^- symmetric stretch with the O–C–O bend and C–C stretch.[17] Nevertheless, if the asymmetric and symmetric COO^- stretches can be identified, the binding geometry of the carboxylate ligand can be derived from the difference in the two, $\Delta\nu_{as\text{-}s}$.[18–20] Specifically, $\Delta\nu_{as\text{-}s}$ should be close to that of the free ionic form, 150 cm^{-1} for $PhCOO^-$, for carboxylates bridging two metal ions, larger in unidentate coordination geometry, and smaller in bidentate mononuclear complexes. As expected, **1a** and **1b** exhibit $\Delta\nu_{as\text{-}s}$ values of 149 and 166 cm^{-1}, respectively, consistent with μ-1,3 bridging carboxylate groups (Fig. S4B). In **1a**·O_2, ν_{as} and ν_s are at 1572/1607 and 1358 cm^{-1}, respectively, and in **1b**·O_2 are at 1550 and 1329 cm^{-1} (Fig. 3A). These frequencies give $\Delta\nu_{as\text{-}s} > 200$ cm^{-1} and suggests a switch from bridging to unidentate coordination for the carboxylate groups in **1a**·O_2 and **1b**·O_2. A bridging carboxylate geometry was demonstrated by X-ray crystallography in a similar (μ-peroxo)diiron(III) species,[21] but facile conversion in carboxylate geometry might occur in solution. Generation of [**1a**·O_2]H^+ and [**1b**·O_2]H^+ is associated with downshift of the ν_{as} modes by at least 20 cm^{-1}, whereas ν_s modes are not observed, possibly shifting below 1300 cm^{-1} (Fig. 3B). Most importantly, the FTIR spectra show no evidence of free carboxylic acid vibrations, i.e. $\nu_{C=O} > 1700$ cm^{-1}.

A comparison of the ^1H NMR spectra of the benzoate and pentafluorobenzoate diiron complexes allows the phenyl ring protons of the former to be identified in **1a**·O_2 as paramagnetically broadened peaks at 7.0, 8.7, and 11.4 ppm (Fig. S5). Upon addition of H[BAr^F_4], these resonances shift to 7.5, 8.0, and 9.8 ppm (Fig. S9), in support of the protonation of the benzoate ligand. This conclusion is confirmed by analysis of the ^{19}F NMR spectra of **2**·O_2 and [**2**·O_2]H^+. The fluorine resonances of the pentafluorobenzoate ring in **2**·O_2 occur at −134.4, −154.4, and −159.0 ppm (Fig. 4A) and shift to −111.3, −143.0, and −154.8 ppm upon addition of 3 equiv of H[BAr^F_4] (Fig. 4B). These results demonstrate that the $C_6F_5CO_2H$ ligand is bound to iron, since the resonances of free pentafluorobenzoic acid appear at −139.5, −150.3, and −162.0 ppm.

In conclusion, the spectroscopic evidence (Table 1) clearly indicate that the carboxylate is preferred over the peroxo ligand as the site of protonation in these (peroxo)diiron(III) model complexes, a possible structure for which is depicted in Scheme 1. Our results suggest that, during the O_2 activation steps in the catalytic cycle of sMMO and related enzymes, protons might generate and/or transform the (peroxo)diiron(III) core by inducing a carboxylate shift,[22,23] possibly increasing the electrophilicity of the diiron unit and facilitating substrate access to the active site. Future work with synthetic analogs will address these important questions.

Supplementary Material

Refer to Web version on PubMed Central for supplementary material.

Acknowledgments

This work was supported by grants GM032134 (S.J.L.) and GM74785 (P.M.-L.) from the National Institute of General Medical Sciences.

References

1. Feig AL, Lippard SJ. Chem. Rev 1994;94:759.
2. Wallar BJ, Lipscomb JD. Chem. Rev 1996;96:2625. [PubMed: 11848839]
3. Vu VV, Emerson JP, Martinho M, Kim YS, Münck E, Park MH, Que L Jr. Proc. Natl. Acad. Sci. U.S.A 2009;106:14814. [PubMed: 19706422]
4. Nordlund P, Reichard P. Annu. Rev. Biochem 2006;75:681. [PubMed: 16756507]
5. Fox BG, Lyle KS, Rogge CE. Acc. Chem. Res 2004;37:421. [PubMed: 15260504]
6. Merkx M, Kopp DA, Sazinsky MH, Blazyk JL, Müller J, Lippard SJ. Angew. Chem., Int. Ed. Engl 2001;40:2782. [PubMed: 11500872]
7. Leahy JG, Batchelor PJ, Morcomb SM. FEMS Microbiol. Rev 2003;27:449. [PubMed: 14550940]
8. Liu KE, Wang D, Huynh BH, Edmondson DE, Salifoglou A, Lippard SJ. J. Am. Chem. Soc 1994;116:7465.
9. Moënne-Loccoz P, Baldwin J, Ley BA, Loehr TM, Bollinger JM Jr. Biochemistry 1998;37:14659. [PubMed: 9778340]
10. Murray LJ, Naik SG, Ortillo DO, García-Serres R, Lee JK, Huynh BH, Lippard SJ. J. Am. Chem. Soc 2007;129:14500. [PubMed: 17967027]
11. Lee S-K, Lipscomb JD. Biochemistry 1999;38:4423. [PubMed: 10194363]
12. Tinberg CE, Lippard SJ. Biochemistry. 2009 In press.
13. Dong Y, Ménage S, Brennan BA, Elgren TE, Jang HG, Pearce LL, Que L Jr. J. Am. Chem. Soc 1993;115:1851.
14. Dong Y, Yan S, Young VG Jr, Que L Jr. Angew. Chem., Int. Ed. Engl 1996;35:618.
15. Jensen KP, Bell CB III, Clay MD, Solomon EI. J. Am. Chem. Soc 2009;131:12155. [PubMed: 19663382]
16. Brunold TC, Tamura N, Kitajima N, Moro-oka Y, Solomon EI. J. Am. Chem. Soc 1998;120:5674.
17. Nara M, Torii H, Tasumi M. J. Phys. Chem 1996;100:19812.
18. Deacon GB, Phillips RJ. Coord. Chem. Rev 1980;33:227.
19. Nakamoto, K. Part B: Applications in Coordination, Organometallic, and Bioinorganic Chemistry. 5th ed.. New York: John Wiley & Sons, Inc.; 1997.
20. Costas M, Cady CW, Kryatov SV, Ray M, Ryan MJ, Rybak-Akimova EV, Que L Jr. Inorg. Chem 2003;42:7519. [PubMed: 14606847]
21. Ookubo T, Sugimoto H, Nagayama T, Masuda H, Sato T, Tanaka K, Maeda Y, Ōkawa H, Hayashi Y, Uehara A, Suzuki M. J. Am. Chem. Soc 1996;118:701.
22. Dunietz BD, Beachy MD, Cao Y, Whittington DA, Lippard SJ, Friesner RA. J. Am. Chem. Soc 2000;122:2828.

23. Rinaldo D, Philipp DM, Lippard SJ, Friesner RA. J. Am. Chem. Soc 2007;129:3135. [PubMed: 17326634]

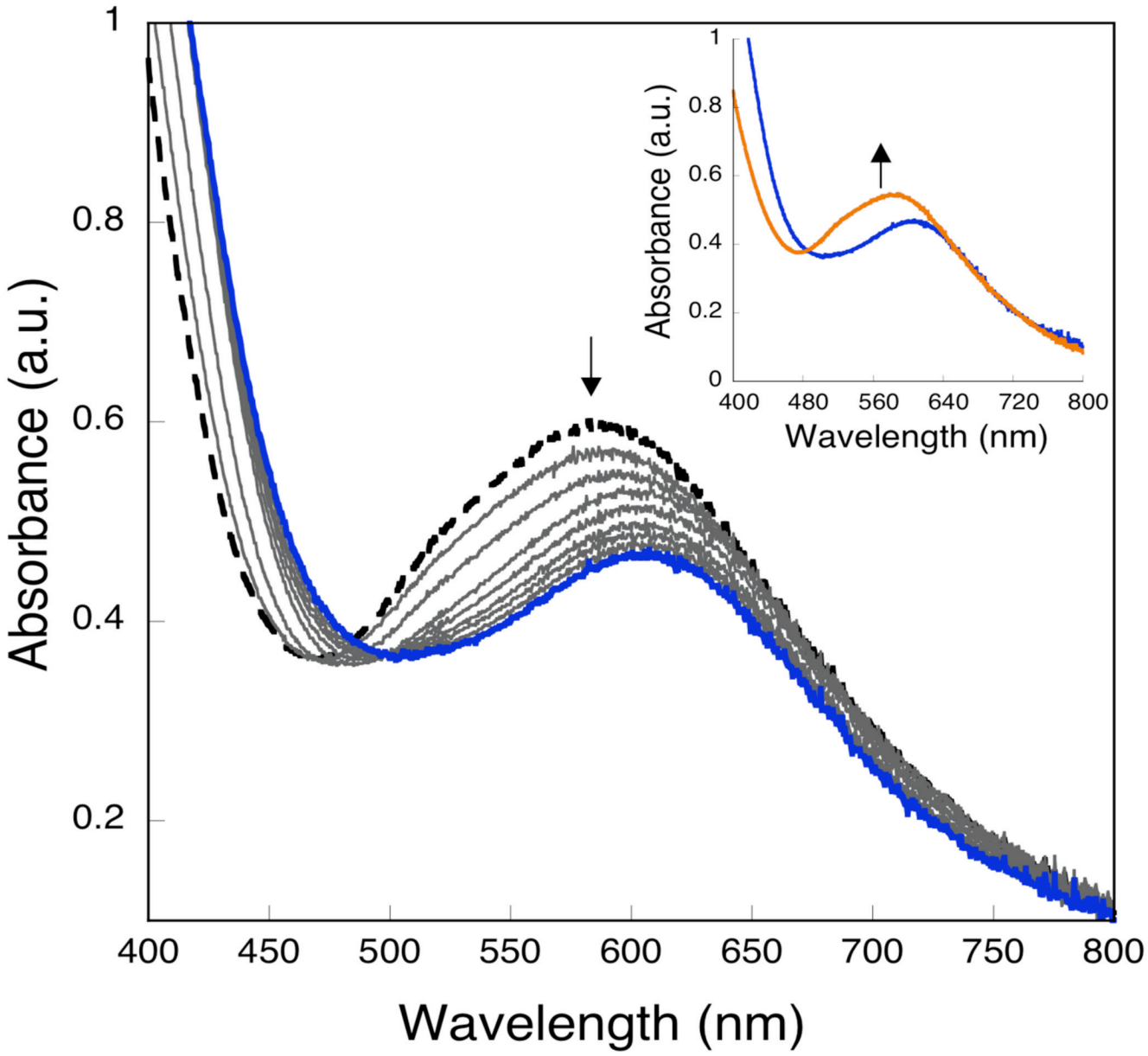

Figure 1.

UV-vis absorption spectra of [**1a**·O_2](BF_4)$_2$ (112 μM in CH_3CN, −30°C, downward arrow) when up to 2.0 equiv of H[$BAr^F{}_4$] were added. Inset: restoration of initial spectrum (orange trace, upward arrow) upon treatment with 2.0 equiv of NEt_3.

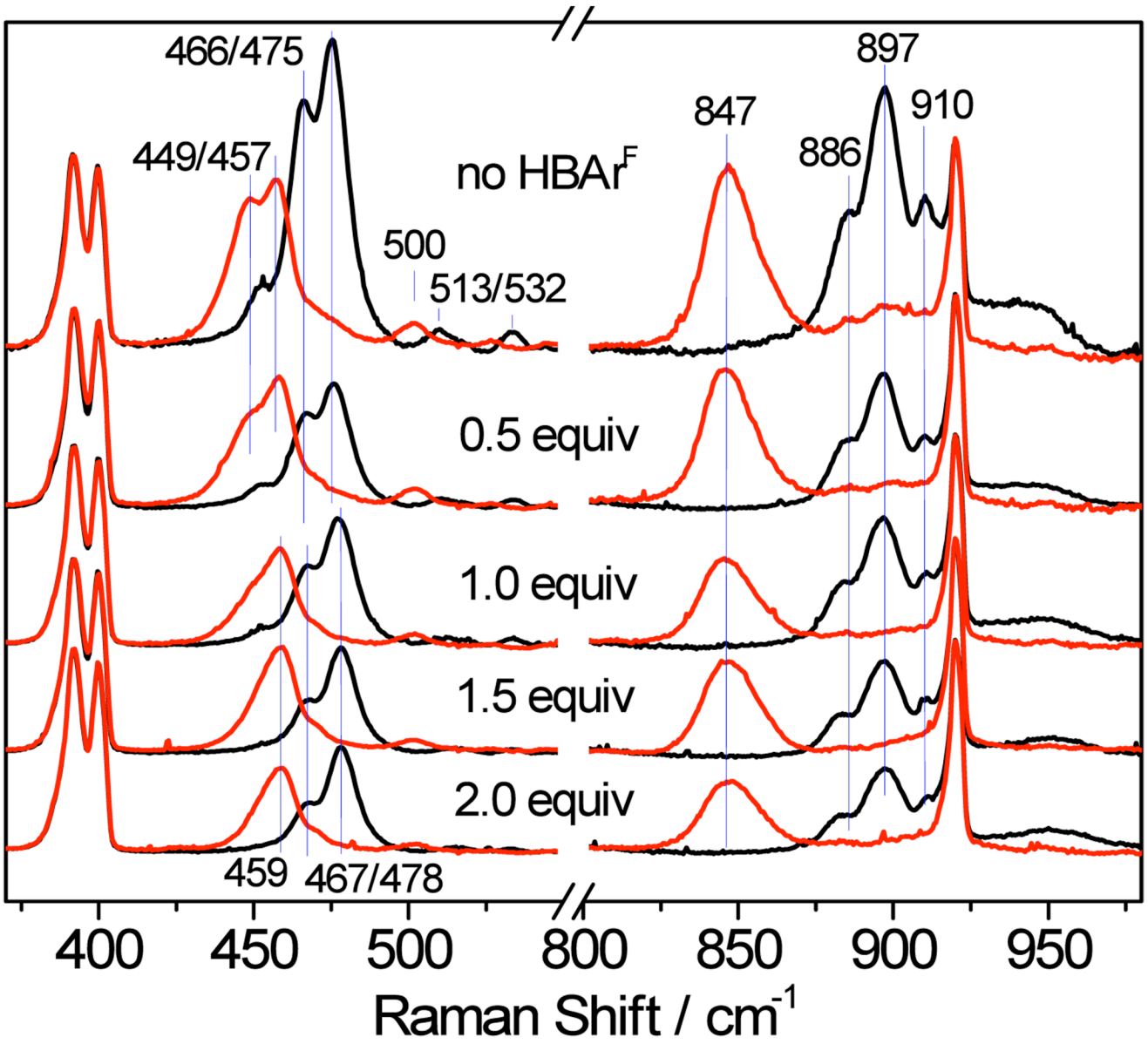

Figure 2.

RR spectra of **2**·$^{16}O_2$ (black) and **2**·$^{18}O_2$ (red) after addition of 0, 0.5, 1.0, 1.5, and 2.0 equiv of H[$BAr^F{}_4$]. Each spectrum was normalized based on the solvent CH_3CN bands at 392, 400, and 920 cm^{-1}.

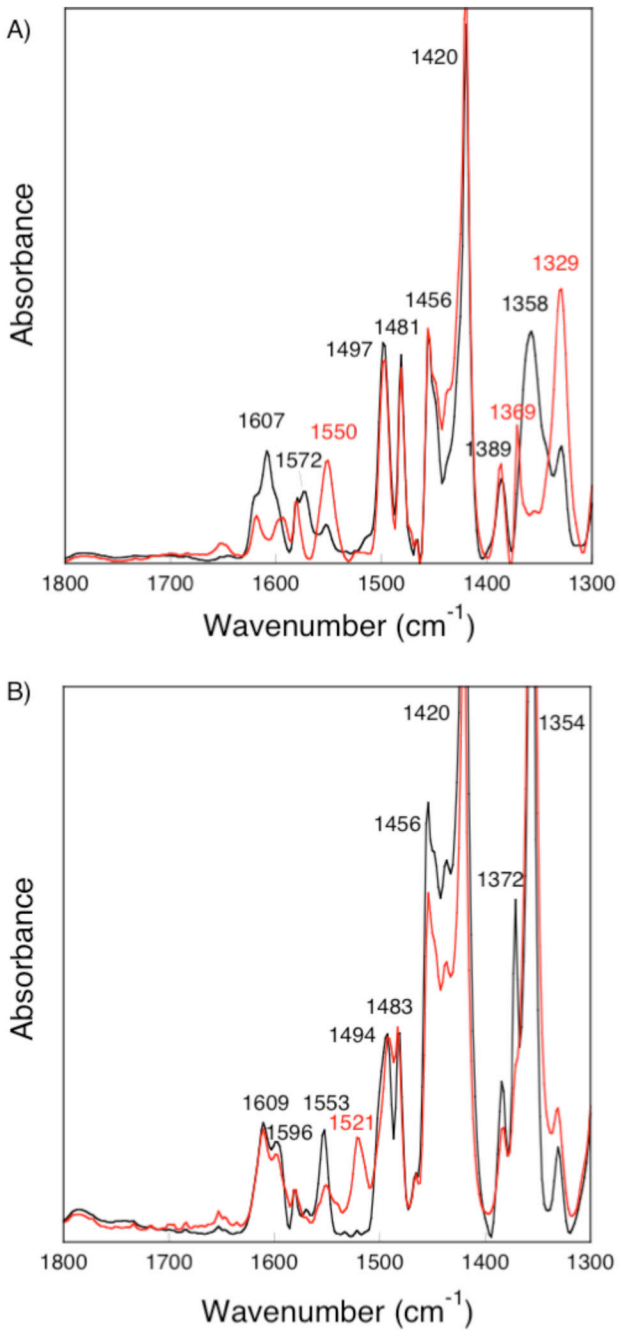

Figure 3.

Solution FTIR spectra of **1a**·O_2 (black) and **1b**·O_2 (red) before (**A**, top) and after (**B**, bottom) the addition of 1.5 equiv of H[BAr^F_4]. The spectra were acquired in CH_2Cl_2 at approx. −30 °C with a diiron concentration of ~55 mM. The intense peaks at 1356 and 1420 cm^{-1} are due to the [BAr^F_4]$^-$ anion and solvent, respectively.

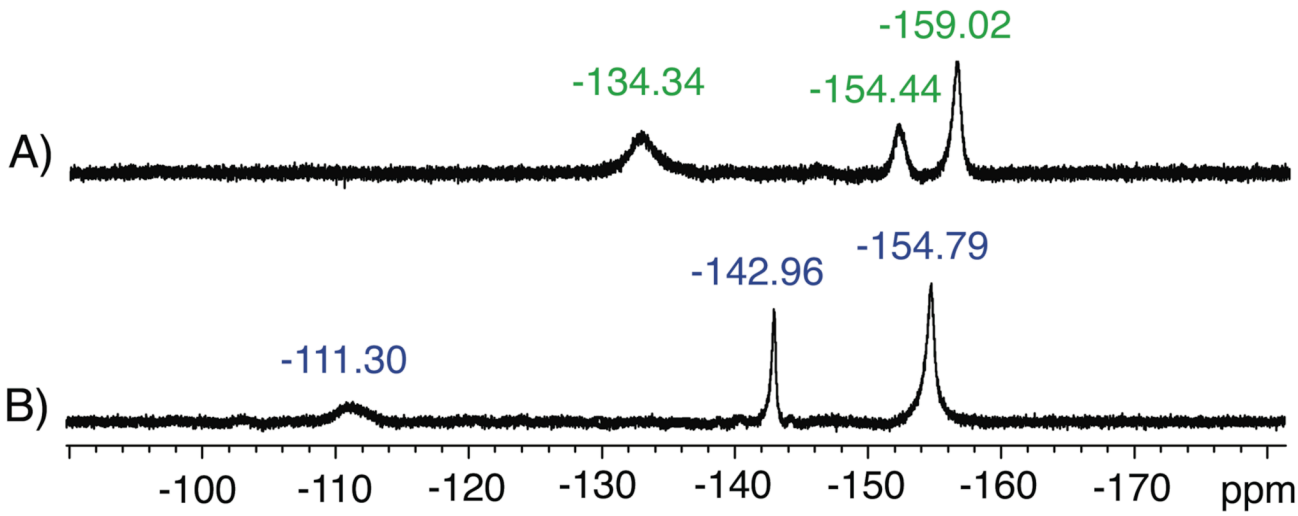

Figure 4.
^{19}F NMR spectra (470 MHz, CD_2Cl_2, −30°C) of [**2**·O_2]$(OSO_2CF_3)_2$ (**A**); and [**2**·O_2] $(OSO_2CF_3)_2$/ H[BAr^F_4] (1:3) (**B**).

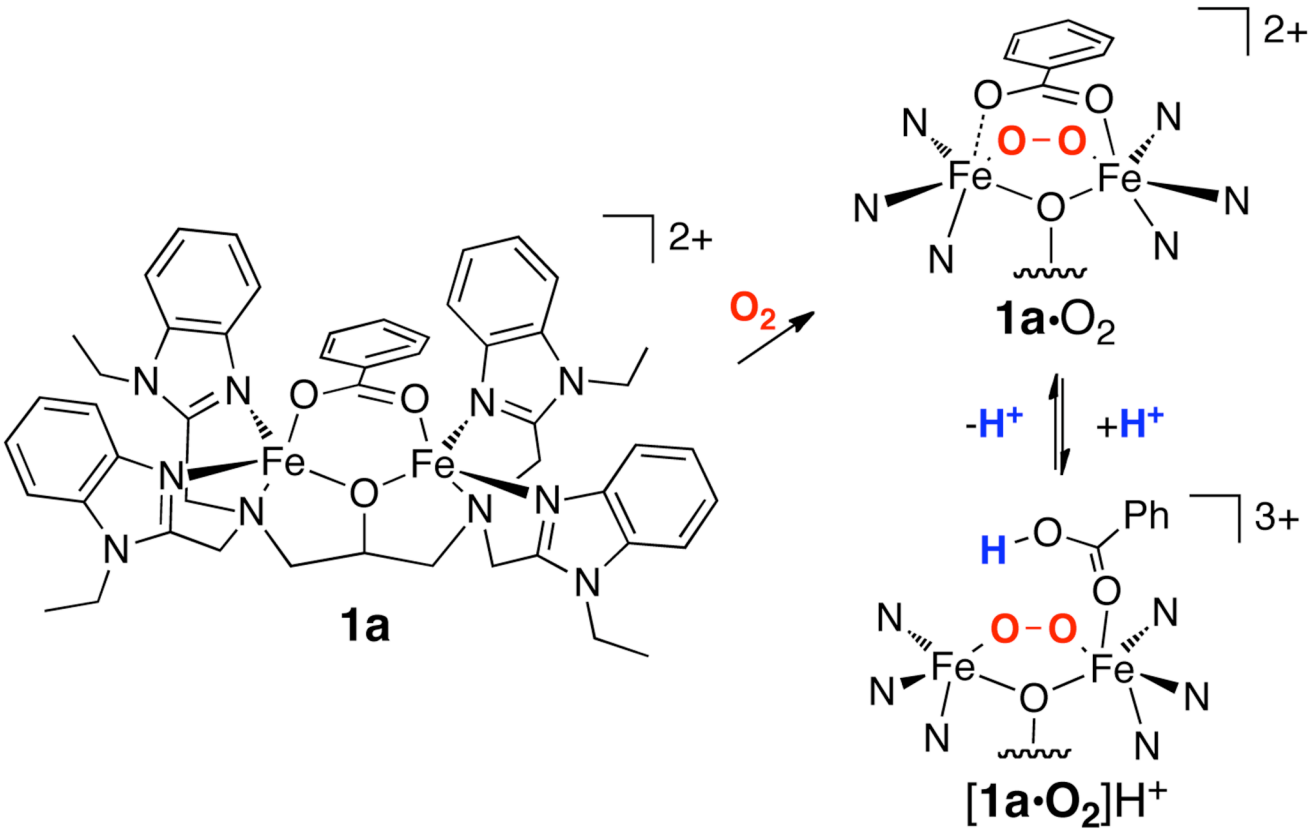

Scheme 1.
Reaction of dioxygen with **1a** and H^+. A possible structure for [**1a**·O_2]H^+ is depicted.

Table 1

UV-Vis, Mössbauer, RR, and FTIR data for **1a**·O_2, [**1a**·O_2]H^+, **1b**·O_2, [**1b**·O_2]H^+, **2**·O_2, and [**2**·O_2]H^+.

Complex	λ_{max}, nm (ε, M^{-1} cm^{-1})	δ, mm/s	ΔE_Q, mm/s	ν (Fe–O), cm^{-1} ($\Delta^{18}O$)	ν (O–O), cm^{-1} ($\Delta^{18}O$)	$\nu_{as}(COO^-)$ cm^{-1} ($\Delta^{13}C$)	$\nu_{s}(COO^-)$ cm^{-1} ($\Delta^{13}C$)	$\Delta\nu_{as\text{-}s}$ cm^{-1}
1a·O_2	590 (3100)	0.53(2)	0.71(2)	466/474 (−18)	897 (−50)	1607/1572 (>−22)	1358 (−29)	>200
[**1a**·O_2]H^+	600 (2360)	0.53(2)	0.80(2)	467/478 (−20)	896 (−53)	1553 (−32)	-	-
2·O_2	600 (3300)	0.53(2)	0.77(2)	466/475 (−18)	897 (−50)	-	-	-
[**2**·O_2]H^+	610 (2700)	0.54(2)	0.84(2)	478 (−19)	897 (−50)	-	-	-